MAX-PLANCK-INSTITUT FÜR PLASMAPHYSIK

GARCHING BEI MÜNCHEN

Approximations in modelling of light-ion reflection in numerical simulations planning for calorimetric measurements

J. Bohdansky and A. De Matteis*

IPP 9/48 June 1984

* ENEA Comitato Nazionale per la Ricerca e per lo Sviluppo dell'Energia Nucleare e delle Energie Alternative, 40138 Bologna

Die nachstehende Arbeit wurde im Rahmen des Vertrages zwischen dem Max-Planck-Institut für Plasmaphysik und der Europäischen Atomgemeinschaft über die Zusammenarbeit auf dem Gebiete der Plasmaphysik durchgeführt.

IPP 9/48

J. Bohdansky
A. De Matteis

Approximations in modelling of light-ion reflection in numerical simulations; planning for calorimetric measurements

(in English) - June 1984

Abstract

The purpose of this report is to study the possibility of using simple beam scattering experiments combined with calorimetric measurements to check the errors introduced in the numerical simulation of the back-scattering event by some common simplifying assumptions. The assumptions examined concern the incidence angle, the exit angle and the energy distribution of the backscattered particles in connection with the energy deposited on a wall bombarded by energetic particles.

Contents

1. Introduction 2

2. Reflection phenomenology and simplifications 3

3. A simple model for energy deposition in a box. 6

4. Numerical results for SS and C 10

5. Influence of angle dependence. 14

6. Influence of energy distribution 18

7. Conclusions. 22

Acknowledgements 23

References. 23

1. Introduction

Numerical simulation of plasma-wall interactions plays an important role in the design of magnetically confined plasma devices. In such calculations it is difficult to make due allowance for the phenomenology of wall interactions, especially backscattering of particles. The reasons are the following: In the first place, very few cases have been closely investigated through experiments, and mostly at energies above 1 keV. In the second place, even when experimental data were available, the phenomenon involves too many parameters to be correctly simulated in a general transport code, where wall interactions are only part of the whole simulation. The normal procedure is then to neglect the influence of some parameters, such as the incident angle, to neglect distributions, such as the energy distribution of backscattered particles, and, moreover, to use theoretically calculated values (e.g. as given by the codes described in /1/ and /2/) when experimental values are not available.

The aim of this study is to discuss the possibility of using simple beam scattering experiments together with calorimetric measurements to check the combined effect of the approximations used for numerically simulating backscattering.

The energy deposition on a box wall bombarded by energetic particles which are reflected from a target in the box is investigated, first in a simple model (Sec. 4) and then in more sophisticated ones (Sec. 5), by using the NIMBUS Monte Carlo neutral transport code /3/. These numerical experiments yield the sensitivity threshold and the resolution of the bolometer required to check the adequacy of the model used and/or the correctness of the theoretically computed data.

A three-dimensional version of the NIMBUS code /4/ was used. The experiments simulated were designed with a view to possibly using a beam of ions with an intensity of 1 mA and an energy of up to 10 keV (hence a power of up to 10 W), like that available at Max-Planck-Institut für Plasmaphysik, Garching (München), together with bolometers having detecting surfaces of about 1 cm^2 and sensitivity in the μW range.

2. Reflection phenomenology and simplifications

The backscattering process, i.e. the chain of events taking place when a particle (ion or neutral) hits a wall, collides with the atoms of the solid and returns to the surface, can be modelled as a transport problem in an amorphous or crystalline medium /1, 2/. In computational models of plasmas surrounded by walls, all these events are simply replaced by reflecting properties of the bombarded surface /5, 6/. These properties depend essentially on the atomic and mass numbers of the projectile and target, and on the incident energy and angle. If the roughness of the surface (perhaps a decisive parameter in the whole process) and the charge state of the reflected particle are neglected, the data for each projectile-target pair, each energy and each incident angle, described below, should be used as a substitute for the processes occurring in the wall.

Let α be the incident polar angle (angle between the incident direction and the normal to the surface) and E_0 the incident energy of the impinging particle. Let, moreover, E be the energy of the reflected particle, β and φ the polar and azimuthal angles, respectively, defining the exit direction. For every projectile-target pair the function

$$p = p\,(E_o,\ \alpha;\ E,\ \beta,\ \varphi)\ , \tag{1}$$

giving the probability of the incoming particle emerging in the element $dE\ d\beta\ d\varphi$ around $E,\ \beta,\ \varphi$, completely characterizes the reflection event for each pair of the parameters $(E_o,\ \alpha)$. The integral probability of a particle being reflected is called the "particle reflection coefficient" and is denoted by $R_N(E_o,\alpha)$. It thus follows by definition that

$$R_N(E_o,\alpha) = \int_0^{E_o}\int_0^{\pi/2}\int_0^{2\pi} p(E_o,\alpha;\ E,\beta,\varphi)\ dE\ d\beta\ d\varphi\ . \tag{2}$$

Coefficient R_N gives the emerging fraction of the impinging particles. The fraction of the incoming energy E_o carried away by the R_N emerging particles is called the "energy reflection coefficient" and is denoted by $R_E(E_o,\alpha)$:

$$R_E(E_o,\alpha) = \int_0^{E_o}\int_0^{\pi/2}\int_0^{2\pi} p(E_o,\alpha;\ E,\beta,\varphi)\cdot\frac{E}{E_o}\ dE\ d\beta\ d\varphi\ . \tag{3}$$

We shall often write R, without subscript, when we refer to both coefficients (2) and (3). Moreover, the shorthand notation $R(E_o)$ will stand for $R(E_o,\ \alpha = 0)$ and thus denotes the reflection coefficients at normal incidence: when we dispense with considering the angle dependence in R and write $R(E_o)$, it will be henceforth understood that the reflection coefficients used are those measured or computed at normal incidence. We shall often use marginal density functions derived from Eq. (1). For example, the probability density function pdf) of the emerging energy

$$f(E_o,\alpha;E) = \frac{\int_0^{\pi/2}\int_0^{2\pi} p(E_o,\ ;\ E,\beta,\varphi)\ d\beta\ d\varphi}{R_N(E_o,\ )}\ , \tag{4}$$

"briefly denoted by $f(E_o;E)$ or $f(E)$ when $\alpha = 0$" or pdf of the exit polar angle

$$h(E_o,\alpha;\beta) = \frac{\int_0^{E_o}\int_0^{2\pi} p(E_o,\alpha;\ E,\beta,\varphi)\ dE\ d\varphi}{R_N(E_o,\alpha)} \qquad (5)$$

In both examples (4) and (5) above, R_N is the normalization factor.

It is immediately seen that the bulk of data (eq. 1) required for faithful simulation of the backscattering is impressive. Simplifications cannot be avoided. A common simplification is the use of the integral quantities given by eqs. (2) and (3) (or, more simply, the use of $R_N(E_o)$ and $R_E(E_o)$ for every incidence angle α) together with a cosine distribution instead of the pdf (5) and an average emerging energy instead of the pdf (4). For example, the simplest model for backscattering adopted in NIMBUS is as follows. When a particle at energy E_o hits a wall, first the reflection event is chosen with probability $R_N(E_o)$. The choice is decided through a random game. If the game is won, the energy E_1 of the backscattered particle is assumed to coincide with the mean energy of the reflected particles

$$E_1 = E = E_o \frac{R_E(E_o)}{R_N(E_o)} . \qquad (6)$$

The exit direction is chosen with uniform azimuth and a cosine distribution for the polar angle. Thus, in this model the target reduces the energy of the reflected particle by a certain amount and only randomizes the direction. At steady state all non-reflected particles are re-emitted at the thermal energy of the target. Reflection coefficients are

given by empirical expressions fitting experimental or theoretical data. Some sophistications of the described model are allowed in special cases, such as introducing a dependence of R_N and R_E on α, or an exit angle with distribution other than the cosine.

Owing to the drastic simplifications used, it seems worthwhile to perform numerical calculations whose results could be experimentally checked in order to judge the interference and the resultant effect of all uncertainties introduced. Another source of uncertainties is due to theoretical data which carry the effects of many assumptions: amorphous or crystalline structure, interatomic potentials, electronic energy losses, type of collision. The deposited energy on the wall was chosen as the quantity to be compared, since it can easily be measured.

3. A simple model for energy deposition in a box

The experiment simulated is as follows: a beam of ions enters a box 10 x 4 x 4 cm from an aperture 0.6 x 0.6 cm located of one of the bases of the parallelepiped and hits a target 1 x 1 cm (Fig. 1). A detector is placed somewhere along the surface AB.

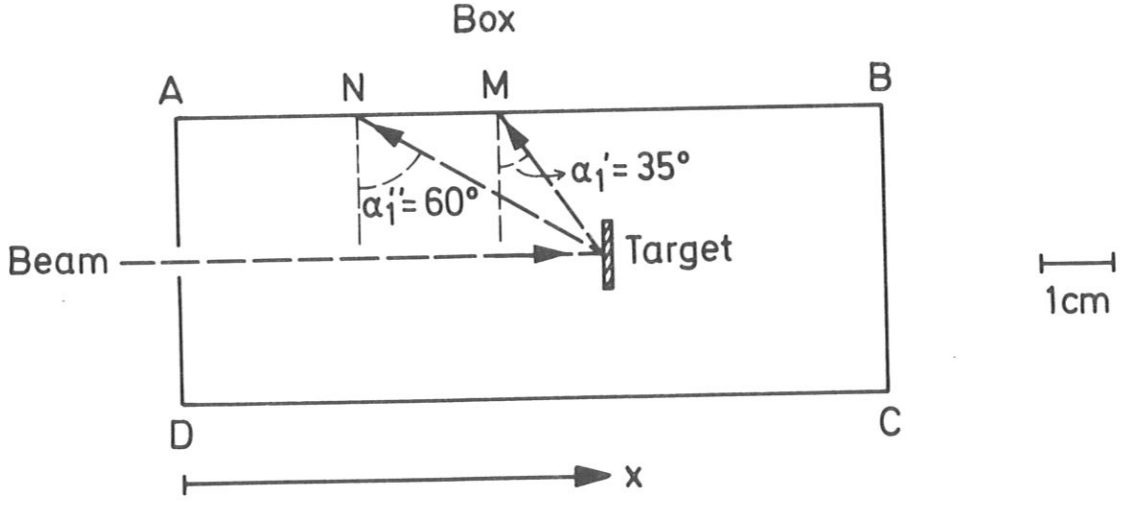

Fig. 1 Experiment simulated (three-dimensional)

The distribution of the thermal load along the box walls will be investigated in various conditions. We shall often use a special material for the target (e.g. tungsten) that is different from that of the box.

The average energy per unit length g(eV/cm) that is deposited per beam particle along the detecting surface AB (which has a height of 4 cm) will be computed. If c is the charge carried per particle and I is the beam current in amperes, then the total power P loading the wall AB per cm is

$$P = g\ [\frac{eV}{cm}] \cdot \frac{I}{c}\ [\frac{A}{e}] = g \cdot \frac{I}{c}\ [w/cm].$$

For a beam current of 1 mA and for singly ionized atoms, the quantity computed will also represent the number of milliwatts deposited per cm by the scattered beam along AB. The power per cm^2, finally, will be P/4 and this will define the sensitivity of the bolometer.

Let E_o be the mean energy of a particle belonging to the beam hitting the target (T) inside the box (B) at normal incidence. In the simple model it is assumed that

1. the escape probability from the box is negligible;
2. the target is small, so that it "disappears" from our balances after the first collision;
3. the coefficients $R_N(E_o)$ and $R_E(E_o)$ are given and there is no dependence $R_N(E_o,\alpha)$, $R_E(E_o,\alpha)$ on incident angle;

4. the law governing the polar exit angle is the cosine; the exit azimuth is uniformly distributed;

5. the energy distribution of the backscattered particles can be neglected and substituted by the average energy (6).

Assumptions 1 and 2 above will only simplify the formalism without introducing relevant errors in the model of the experiment described in Fig. 1. Much more important are assumptions 3 to 5, with which we try to replace the knowledge of the probability function (1).

We shall begin with balances extended to the whole box. The energy Q_n deposited on the surfaces at the n-th collision by the particle considered, and the mean energy E_n of the particle (ion or neutral) after the n-th collision can be recursively defined by starting from

$$Q_1 = E_o - E_o\, R_E^T(E_o) = E_o[1-R_E^T(E_o)], \qquad +)$$

$$E_1 = E_o \frac{R_E^T(E_o)}{R_N^T(E_o)}$$

$$Q_2 = E_o\, R_E^T(E_o) - [E_o\, R_E^T(E_o)]\, R_E^B(E_1) = E_o\, R_E^T(E_o)\, [1-R_E^B(E_1)] ,$$

$$E_2 = E_1 \frac{R_E^B(E_1)}{R_N^B(E_1)} ,$$

+) For Q_1 recombination energy and ionization energy is neglected. For Q_2 only recombination energy is neglected as the reflected particles are neutral.

and recalling that after the second collision only superscript B survives (T and B denote the target and box material, respectively.

If cut-off is assumed at 0.1 eV, the above definitions can be completed by adding the following

$$Q_i = 0 \quad \text{whenever } E_i \leq 0.1 \text{ eV}.$$

The energy deposited on the box wall per beam particle is then

$$Q = \sum_{2}^{\infty} Q_i \ ,$$

and multiplied by the particle flow gives the total power deposited on the box walls.

When the balances with the detector covering only a small fraction of the box wall are rewritten and the contributions upon this restricted area are now denoted by q_i ($\sum_i q_i = q$), we have for the contribution q_2 on the detector

$$q_2 = a_{12} Q_2 \ ,$$

where q_{12} is the fraction of the total energy $E_o R_E(E_o)$ directly reflected from the target to the detector. Subscripts recall the transition from the first to the second collision. In our simple model the coefficient a_{12} depends solely on the geometry of the experimental set-up.

4. Numerical results for SS and C

A. Stainless steel

Figures 2 and 3 give the results obtained with the assumptions 3 to 5 of Sec. 3 when the box material is stainless steel and the target is of the same material or tungsten. Empirical formulas at normal incidence, proposed in /6/, were used for the reflection coefficients of

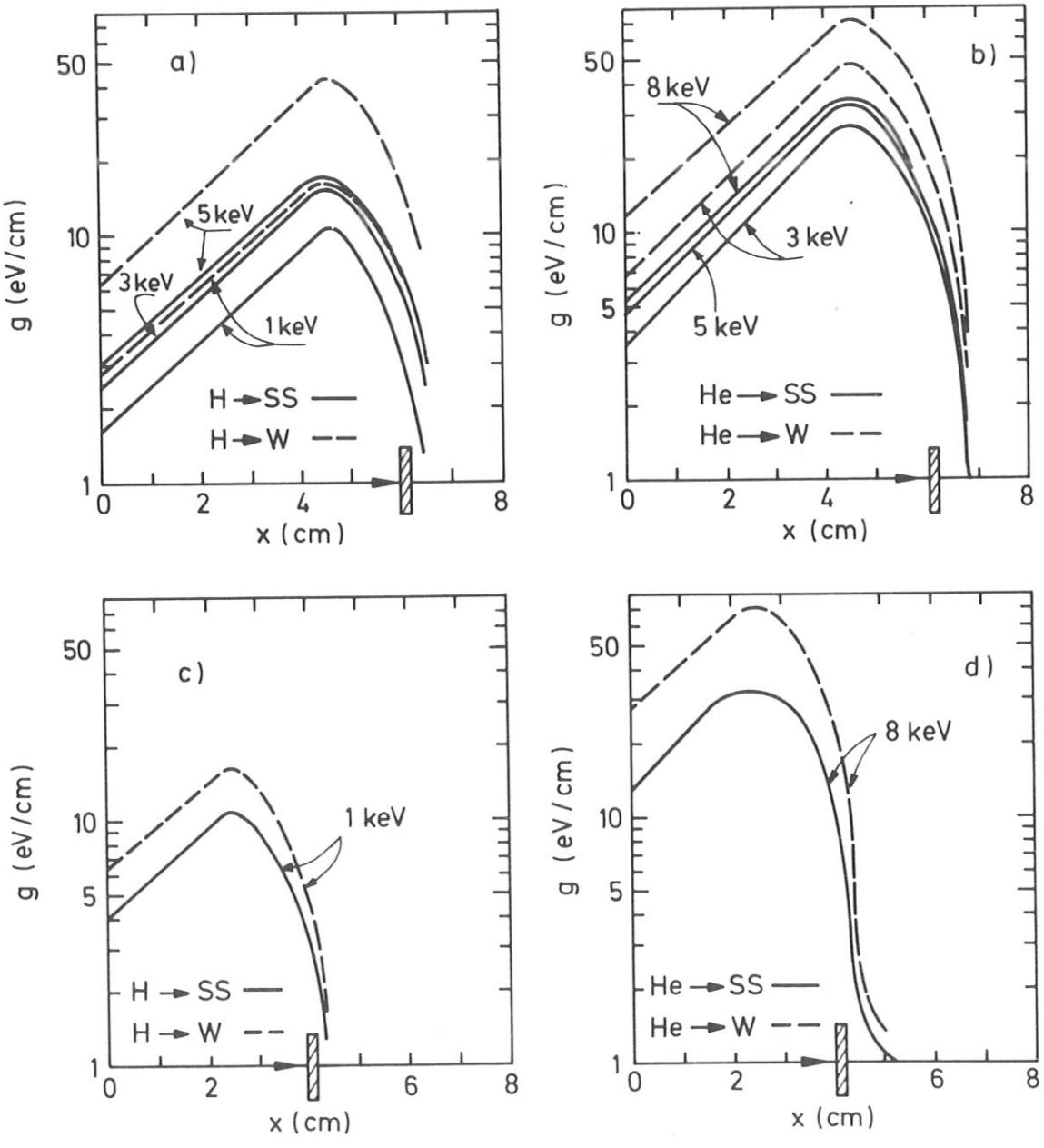

Fig. 2 Energy deposited along the SS surface AB per beam particle (H or He)
a) and b): target (SS or W) at 6 cm from the beam entrance
c) and d): target (SS or W) at 4 cm from the beam entrance.

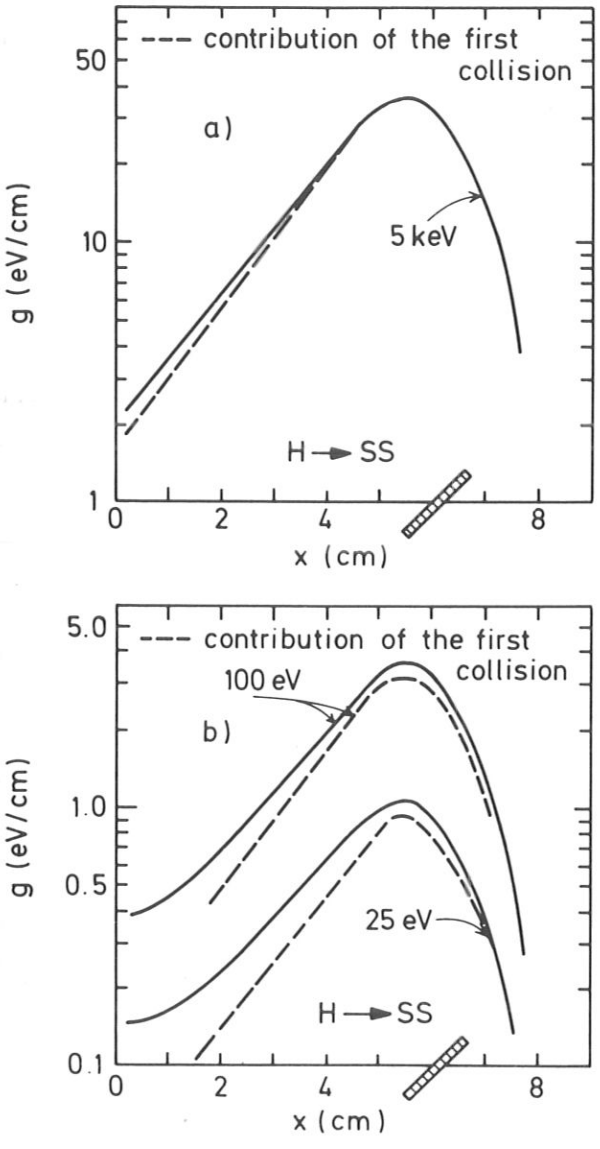

Fig. 3:
Energy deposited along the SS surface AB per beam particle. SS target, incidence angle 45^{o}.

the first material. For tungsten universal formulas, given in /3/, were adopted. The ion energy and the ion species investigated are quoted for each case. The position of the target is also shown in the figures. In Fig. 2 the target is normal to the beam, while in Fig. 3 the incidence angle is 45^{o}. We shall first comment on the results of Fig. 2. The first two cases, a) and b), with the target 6 cm from the entrance of the beam into the box, show that for the ions, beam energy and target used the profiles of the energy deposited are similar. Within the model, they

only depend on the geometry adopted and can be characterized by a maximum at about 1.5 cm from the target (point M in Fig. 1), the right wing rapidly decreasing and the left wing decreasing almost exponentially. The statistical error of the maximum value of g (depending on the number of histories run) is about 3 %. The angle α_1, corresponding to g_{max}, is

$$\alpha_1 \ (g_{max}) \simeq 35^{o}.$$

A tungsten target enhances for both H and ^{4}He the energy deposited at the maximum without changing the nature of the curve.

Many facts indicate a dominance of the first collision with the box wall in the results. For example, the distance between the target and entrance hole (Fig. 2c and 2d) is reduced, the profile simply shifts to the left together with the target, and the left wing is thus insensitive to contributions coming from neighbouring walls by multiple collisions, i.e. $q \simeq q_2$. This can be checked in Fig. 3, where the contribution of the first collision with the box wall is given separately. To enhance the small effect, the target here was turned 45^{o} in order to concentrate (and more easily compute) the reflected beam upon the test wall (in fact, the maximum is doubled). Only by decreasing the beam energy, as in Fig. 3b, is some effect achieved both in the maximum ($\simeq$ 10 % at 25 eV) and in the left wing, where the contribution of other walls is now felt. The angle corresponding to the new maximum is here

$$\alpha_1 \ (g_{max}) \simeq 10^{o},$$

i.e. it has rotated together with the target according to the assumptions.

From Figs. 2 and 3 it can be concluded that the contribution of other collisions after the first one on the box wall seems negligible for $E_o \geq 1$ keV and is only 10 % around the maximum for E_o = 25 eV. Moreover, a 1 mA beam of 1 keV protons hitting an SS box surface deposits a maximum power of about 2 mW/cm^2, which is well above the sensitivity threshold of the available detector. For a 1 mA beam of 25 eV (Fig. 3b) the deposited power is also well above this threshold. The resolution should be sufficient to discern the difference between the total and the contribution of the second reflection.

B) Graphite

Specific data given in /5/ were approximated as described in /3/ for our simulations. Some of these data derive from experiments, many others from theoretical computations. As very few results are available for He, the computed reflection coefficients of tritium as a function of the reduced energy were used instead.

Figure 4 plots the maximum of g, in the case of a graphite box and a tungsten target, as a function of beam energy for H and He and normal ion incidence. The position of the maximum is the same as in the previous section. The contribution of the first collision against the box wall seems here almost coincident with g (see Fig. 4b) in the case of hydrogen, while no difference at all between g and g_1 was observed for helium.

With a beam current of 1 mA the calculated power deposition, $g_{max}/4$ [mW/cm^2], is well above the threshold sensitivity of the available bolometer.

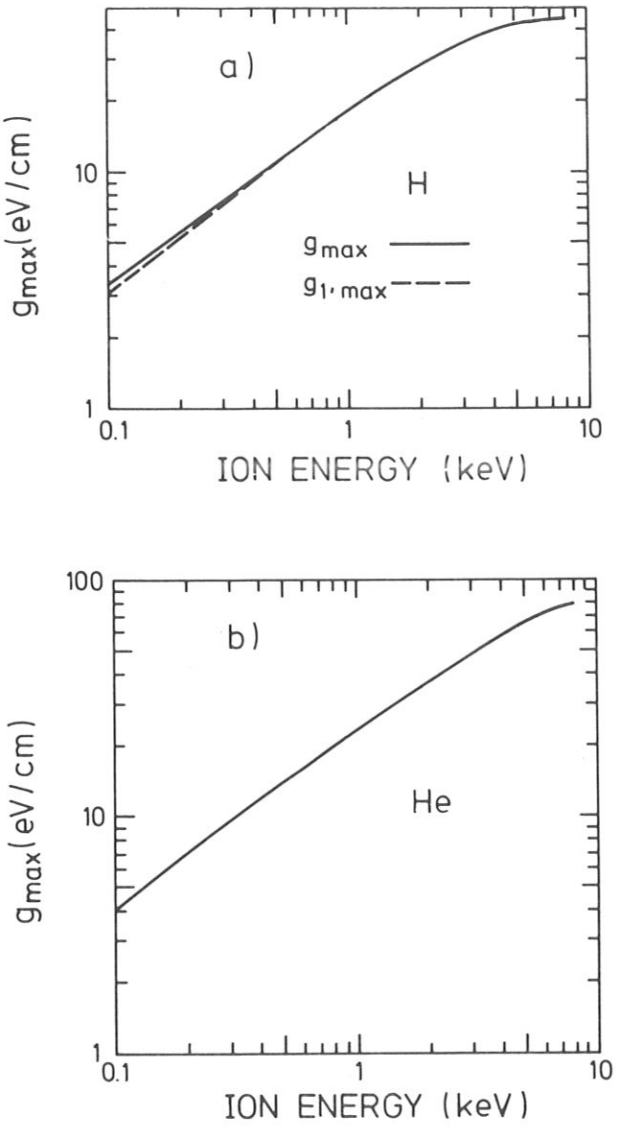

Fig. 4

C box, W target. Maximum energy deposited on the graphite surface AB per beam particle (H or He) vs. ion energy

5. Influence of angle dependence

An experiment like that planned in the previous section could check the cumulative effect of all simplifying assumptions made. It is not unreasonable to hope that there will be some compensation between the various neglected effects in the case of multiple collisions. It will be shown here that, in a more sophisticated model as far as the angle de-

pendence is concerned, this compensation does in fact take place.

We shall now drop restriction 3 of Sec. 3 relating to the angle dependence of the reflection coefficients, maintaining the box of Fig. 1, and try to analyze the effect of this angle dependence on the energy deposited.

Oen and Robinson /7/ have numerically evaluated the dependence of reflection coefficients on the incidence angle for hydrogen and helium bombarding a copper surface. According to their results both the coefficients are enhanced with respect to normal incidence, e.g. by a factor of about 1.4 for $\alpha = 45^{o}$ and for 1 keV protons. This effect increases at higher incidence angles and at lower energies.

Results /7/ for hydrogen on copper were approximated in our computations as follows (α is now in radians):

$E_o \leq 2$ keV

$$R_N^{Cu}(E_o,\alpha) = R_N^{Cu}(E_o,0)\,[0{,}597\ \alpha^2 - 0{,}007\ \alpha + 1]$$

$$R_E^{Cu}(E_o,\alpha) = R_E^{Cu}(E_o,0)\,[0{,}405\ \alpha^2 + 0{,}446\ \alpha + 1]$$

$E_o > 2$ keV

$$R_N^{Cu}(E_o,\alpha) = R_N^{Cu}(E_o,0)\,[1{,}807\ \alpha^2 - 0{,}250\ \alpha + 1]$$

$$R_E^{Cu}(E_o,\alpha) = R_E^{Cu}(E_o,0)\,[5{,}320\ \alpha^2 - 1{,}531\ \alpha + 1].$$

Figure 5 gives the distribution of the energy deposited along the Cu surface AB with and without angle dependence. It is seen that when the incidence angle is taken into account, the energy profiles assume a slightly new character: the left wing is no longer the "exponential" found without angle dependence of the reflection coefficients and the maximum is lower. The average number n of collisions undergone by a beam particle with the surface AB before thermalization is also given for each profile.

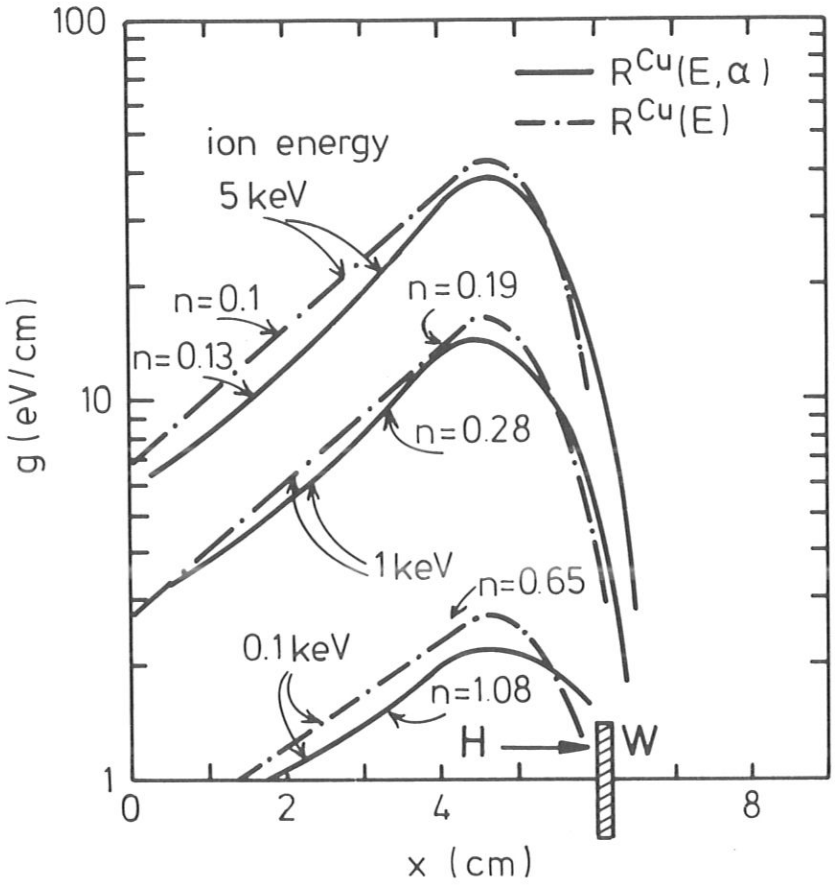

Fig. 5 Cu box, W target. Energy deposited along the surface AB per beam particle (H), with (——) and without (—·—) angle dependence in $R^{Cu} \cdot n$, average number of collisions per beam particle.

Figure 6 gives the energy densities g at the two points M and N of Fig. 1, corresponding to the incident angle $\alpha_1' = 35^o$ (maximum of g) and $\alpha_1'' = 60^o$ (2 cm to the left of the maximum), respectively, versus ion energy. The results obtained with and without angle dependence confirm that the energy deposited is but little influenced by the law taking into account the incidence angle. A decrease of only about 10 % is observed for the beam energy $E_o = 1$ keV.

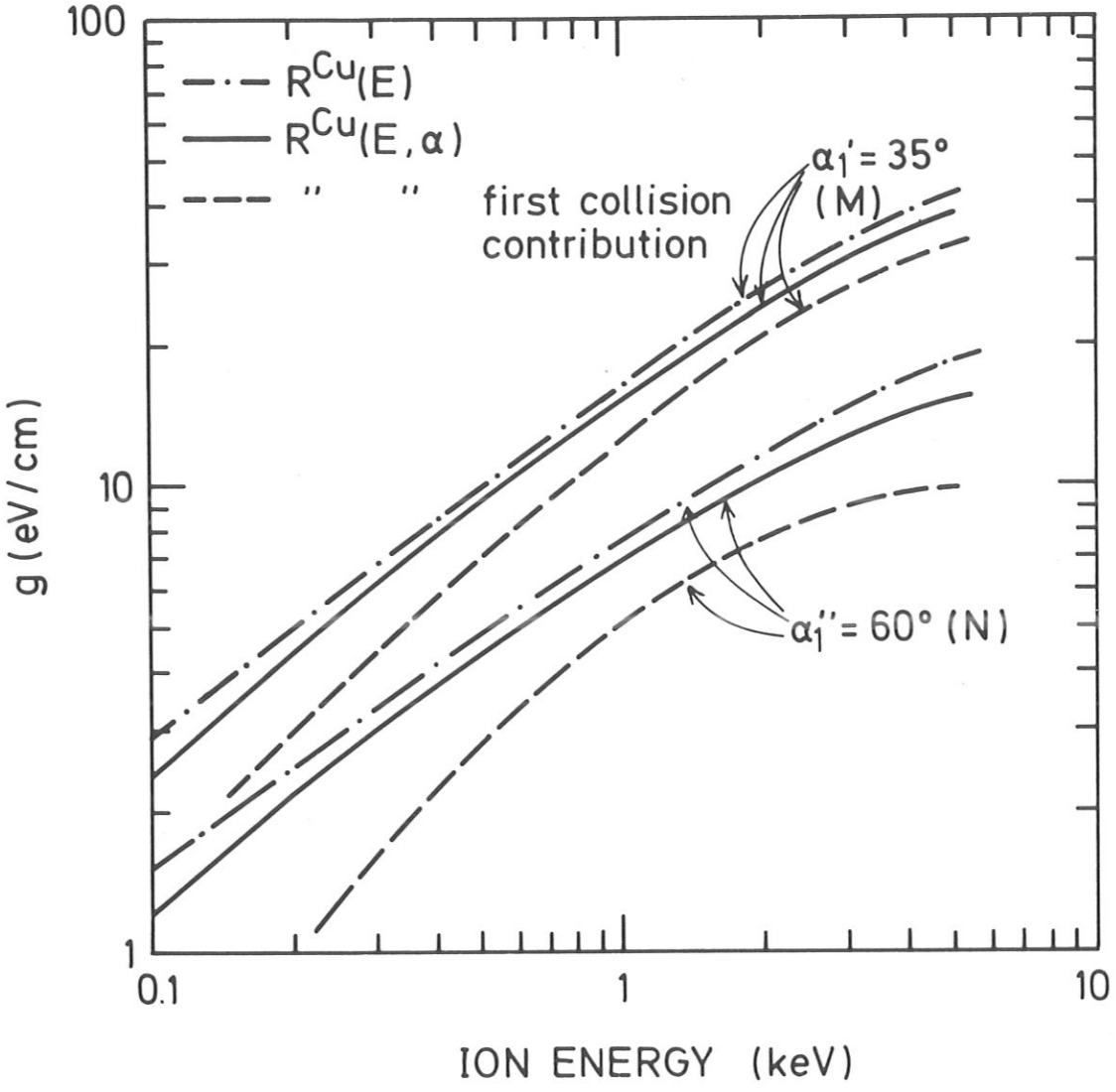

Fig. 6 Cu box, W target. Energy deposited per cm and beam particle (H) at points M and N of Fig. 2 vs. ion energy, with (——) and without (—·—) angle dependence in R^{Cu}. Contribution of the first collision (---) in M and N with angle dependence.

The smallness of this effect for large incidence angle, too, is an interesting feature and can be explained as follows. Both the reflection coefficients increase with the incidence angle, i.e.

$$R_N(E_o,\alpha) \geq R_N(E_o,0) = R_N(E_o) ,$$

$$R_E(E_o,\alpha) \geq R_E(E_o,0) = R_E(E_o) .$$

In the case of angle dependence, at each collision the amount of reflected energy increases and therefore the deposited energy decreases. The fact that the final difference is not significant can be explained by the increased number of collisions (shown in Fig. 5), which almost completely compensates the other effects. The dash-and-dot lines in Fig. 6, which give the contribution of the first collision on the copper wall when the angle α is taken into account, show in fact that in this experiment the first collision on the copper wall is still important, but no longer predomates over the successive contributions. The more frequent collisions, in turn, reduce the difference.

6. Influence of energy distribution

In order to isolate and critically discuss assumption 5 (Sec. 3) on the energy distribution (4) of the emerging particles, f(E), we now turn to the case of normal incidence for the first two collisions. In this case, reflection coefficients used in the numerical model (assumption 3) and also the cosine distribution (assumption 4) are,in fact,fairly well confirmed experimentally.

The effect of the energy distribution could be studied in a spherical box or, better, still by the arrangement given in Fig. 7. In this way, the effect of further collisions (after the first two on target T_1 and T_2) is minimized. By rotating the second target T_2 around T_1, it is possible to isolate and measure the total contribution of the first collision on the spherical surface, Q_2'. Finally, it is assumed that the two targets, T_1 and T_2, are of the same material.

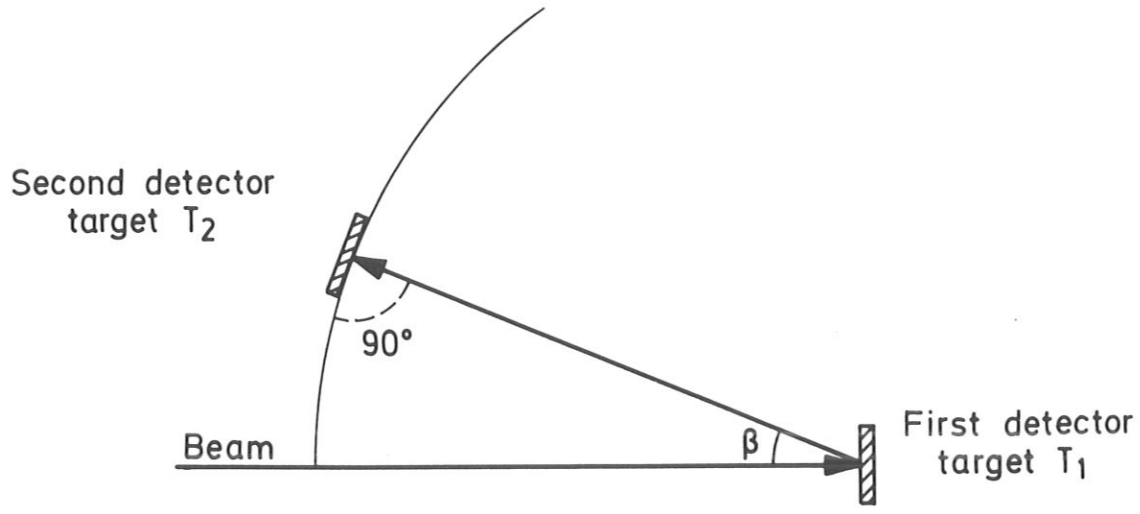

Fig. 7 Set-up for two normal collisions

Thus, let the energy E of the particles emerging from the first collision with the target T_1 now be a random variable with pdf (4),

$$f(E_o, \alpha = 0; E) = f(E).$$

The energy reflected at the second collision for each impinging particle having energy E is $E\, R_E(E)$. Since the number of particles emerging per incident particle from the first collision around E is $R_N(E_o)f(E)dE$, the total energy reflected per beam particle at the second collision is

$$R_N(E_o) \int_0^{E_o} E\, R_E(E)\, f(E)dE = R_N(E_o) < E\, R_E(E) >.$$

Thus, the second contribution Q_2' to the energy deposited is now

$$Q_2' = E_o\, R_E(E_o) - R_N(E_o) < E\, R_E(E) > .$$

By using Eq. (6), this last quantity can be written

$$Q_2' = E_o \, R_E(E_o) \left[1 - \frac{< E \, R_e(E) >}{<E>}\right] , \qquad (7)$$

where

$$<E> = \int_0^{E_o} E \, f(E) dE \ .$$

The second contribution Q_2, computed in Sec. 3 with the different assumption that all emerging particles had the same average energy $<E>$ given by Eq. (6), was

$$Q_2 = E_o \, R_E(E_o) \left[1 - R_e(<E>)\right] ;$$

the error $Q_2 - Q_2'$ introduced by omitting the energy distribution of the reflected particles therefore depends on the difference

$$\Delta = <E \, R_E(E)> - <E> R_E(<E>) ,$$

i.e. on the difference

$$\Delta = <F(E)> - F(<E>) ,$$

with

$$F(E) = E \, R_E(E) .$$

A sufficient condition to get $\Delta = 0$ is that the function F be linear. In this case, whatever the profile f(E), the correctness of a distribution F(E) could not be checked by our calorimetric measurement of Q_2', since the second distribution would coincide with that yielded by the δ-distribution (6). The influence of a distribution f(E) on Q_2' cannot be made evident as long as the linearity condition holds.

The function F, given in terms of the "reduced" energy ε, is universal and has a maximum around $\varepsilon = 1.5$, with monotonic behaviour before and after this maximum. Figure 8 plots the function $F(\varepsilon)$ at the left of the maximum. If the important part of the distribution f(E) occurs in an interval where $F(\varepsilon)$ can be approximated by a straight line, the error will not be relevant. This has been checked for the case of deuterium hitting a nickel target at 300 eV ($\varepsilon \simeq 0.1$). According to the data quoted in /6/, Figs. 2.5 and 2.14, it is found that

$$\langle E\ R_E(E)\rangle = 51.4 \text{ eV},$$

while

$$\langle E\rangle\ R_E(\langle E\rangle) = 50 \text{ eV}.$$

The difference of 3 % confirms the virtual linearity of F(E) in the range examined ($0 < \varepsilon < 0.1$), and therefore Q_2' is not sensitive to f(E).

It may be concluded that, as far as the energy deposited on walls is concerned, the energy distribution f(E) seems to have but little influence. It may also be added that at low energies the computed distributions f(E) show a tendency to a sharper peak (/6/, Fig. 2.14), so that approximation (6) adopted in NIMBUS is quite justified in this range. Of course, we are aware that the replacement of an energy distribution by a constant energy could preserve the thermal load on a wall, but not other quantities such as reaction rates or mean free path or ionization length reflected particles in the plasma.

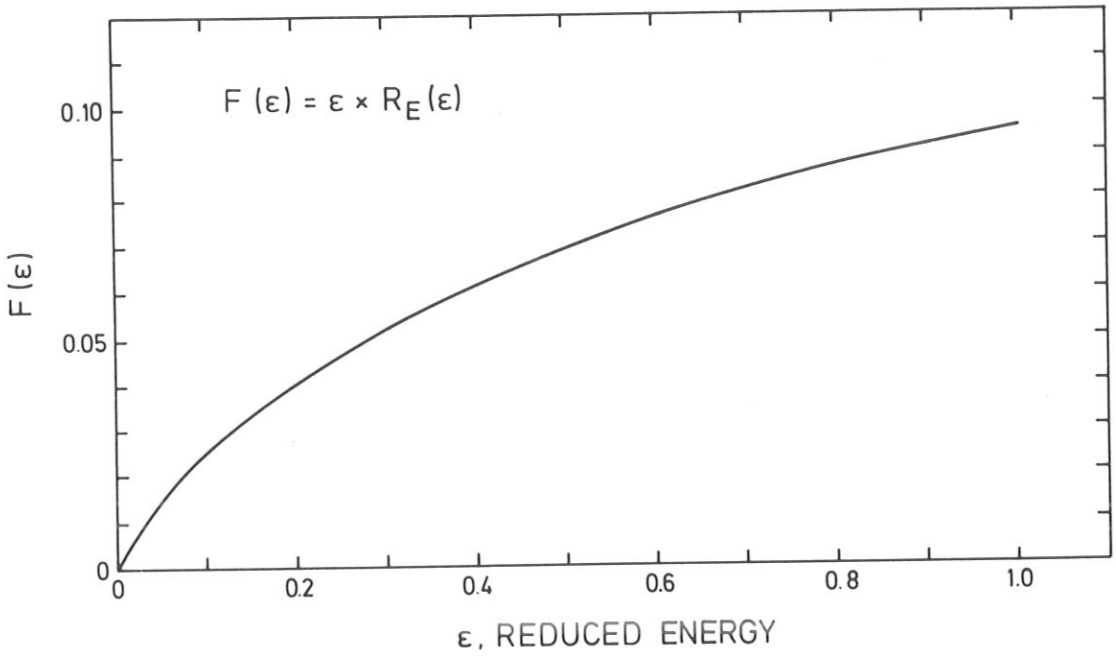

Fig. 8 The universal function $F(\varepsilon)$ from $\varepsilon = 0$ to $\varepsilon = 1$.

7. Conclusions

The explorative computations performed here seem to show that a bolometer with sensitivity 1 $\mu W/cm^2$ could be used in order to estimate the error introduced by current simplifications of the backscattering event in the computed thermal load of a wall bombarded with energetic particles.

In a parallelepiped box with multiple collisions the cumulative effect of these simplifications could be experimentally evaluated. The sensitivity analysis performed for the case of strong dependence of the reflection coefficients on the incident polar angle showed that, fortunately, there is some compensation between effects often neglected in the numerical models when multiple collisions occur.

The influence of the energy distribution of the reflected particles was discussed by isolating its effect in a spherical box with the first two collisions at normal incidence. This effect was found to be rather modest on the energy deposited on a wall, and thus difficult to be experimentally detected.

If the same experiments discussed in this work could be repeated with a bolometer having a rough detecting surface, thus being closer to the operating conditions of plasma devices, the interest would be increased.

Acknowledgements

This work was partly supported by the European Atomic Energy Community and the Euratom-ENEA Association, under contract No. 127/83-1/FU-I/NET.

References

/1/ M.T. Robinson, I.M. Torrens, Phys.Rev. B9 (1974) 5008

/2/ J.P. Biersack, L.G. Haggmark, Nucl.Instr.Meth. 174 (1980) 257

/3/ E. Cupini, A. De Matteis, R. Simonini "NIMBUS-Monte Carlo simulation of neutral particle transport in fusion devices" NET-report Nr. 9 EUR XII-324/9 (1983)

/4/ E. Cupini, A. De Matteis, R. Simonini (in preparation)

/5/ W. Eckstein, H. Verbeek, "Data on light ion reflection" Max-Planck-Institut für Plasmaphysik, Garching b. München, Report IPP 9/32 (1979)

/6/ W. Eckstein, H. Verbeek, to be published in Nucl. Fusion (1984)

/7/ O.S. Oen, M.T. Robinson, Nucl.Instr.Meth. 132 (1976) 647.